Article

Porous Thermoplastic Molded Regenerated Silk Crosslinked by the Addition Of Citric Acid

Alessio Bucciarelli * , Nicola Vighi , Alessandra Maria Bossi , Brunella Grigolo , Devid Maniglio

Posted Date: 4 January 2023

doi: 10.20944/preprints202301.0058.v1

Keywords: Bone Tissue Engineering; Bone Scaffold; Citric Acid; Silk Resin; Compression Molding

Article

Porous Thermoplastic Molded Regenerated Silk Crosslinked by the Addition of Citric Acid

Alessio Bucciarelli [1,*], Nicola Vighi [2], Alessandra Maria Bossi [3], Brunella Grigolo [4] and Devid Maniglio [5,*]

[1] Laboratorio RAMSES, IRCCS Istituto Ortopedico Rizzoli, Via di Barbiano 1/10, 40136 Bologna, Italy; alessio.bucciarelli@ior.it; brunella.grigolo@ior.it
[2] Vetrodomus S.P.A., Via G. Bormioli 48, 25135 Brescia, Italy; n.vighi@vetrodomus.it
[3] Department of Biotechnology, University of Verona, Strada Le Grazie 15, Verona 37134, Italy; alessandramaria.bossi@univr.it
[4] Department of Industrial Engineering, BIOtech Research Center, University of Trento, Via delle Regole 101, Trento 38123, Italy; devid.manglio@unitn.it
* Correspondence: alessio.bucciarelli@ior.it

Abstract: Thermoplastic molded regenerated silk was proposed as structural material in tissue engineering applications, mainly for application in bone. The protocol allows to obtain a compact non-porous material with a compression modulus in the order of a Giga Pascal starting from silk fibroin by compressing a silk fibroin lyophilized sponge of powder in mold at temperature higher than the glass transition temperature (T_g). The main purpose of the produced resin was the osteofixation and other structural applications in which the lack of porosity was not an issue. In this work, we introduced the use of citric acid in the thermoplastic molding protocol of SF to obtain a porosity inside the structural material. In addition to the previously developed protocols the addition of citric acid allowed us to obtain a structural material. The CA powder during the compression acted as a template for the pore formation. In addition, the CA was able to effectively crosslink the SF chain improving the mechanical strength. This effect was proved both evaluating the compression modulus and by studying the spectra obtained by Fourier infrared spectroscopy (FTIR). This protocol may be applied in the near future to the production of a structural bone scaffold.

Keywords: bone tissue engineering; bone scaffold; citric acid; silk resin; compression molding

1. Introduction

Silk Fibroin is the internal structural protein of the silk bave and is responsible to its high mechanical strength. Structurally silk fibroin has a semi-crystalline structure in which the β-sheet crystallites are rigid and mechanically resistant (highly ordered amino acid sequence, heavy chain, 300kDa) and the amorphous phase (random coil secondary structure, light chain, 25kDa) is flexible[1]. The unfolding of the β-structures during the protein dissolution and the possibility to tune their refolding allows to change the material properties. This tunability, combined with the extreme versatility to be processed in mild conditions to obtain a wide range of architectures and its affinity to biological tissues, has made silk fibroin a perfect candidate for tissue engineering (TE) applications[1–4].

In bone tissue engineering (BTE) fibroin is used to develop biomimetic architectures with a porous structure[5–8] Several strategies have been adopted, including but not limited to freeze-drying[9–11], salt-leaching[9,12,13], foaming[14–16]. In almost all of them the mechanical stability is ensured by the folding of the secondary structure into β-sheets in a mechanism that is known as physical crosslinking[17,18]. Only a method was reported bases on a chemical crosslinking of a methacrylated version of silk fibroin (methacrylated silk, Sil-MA)[14]. The main issue with fibroin

Preprints (www.preprints.org) | NOT PEER-REVIEWED | Posted: 4 January 2023 doi:10.20944/preprints202301.0058.v1

scaffolds is their mechanical strength that is far from the natural bone. This does not allow their use in structural applications in which a mechanical bearing is applied.

The only fibroin structures developed for BTE reported to have high mechanical performances are resins[19–24]. These resins have a compact non-porous structure suitable for structural applications but mainly intended for osteofixation due to the lack of a biomimetic architecture. Two main methods are use in literature to produce them. The first is a sol-gel-solid transition from the denaturated protein in water or from a fibroin solution in hexafluoro isopropanol[25]. The solvent evaporation gradually allows the formation of a gel and then of compact solid material. However, this method requires a discrete amount of time to complete the evaporation and a second step to model the required object by subtractive manufacturing[25].

The latter method consists in a solid-solid transition obtained from a compression molding of a lyophilized fibroin sponge[23] or a fibroin powder[26] with a low crystallinity. To set an appropriate process several parameters need to be controlled. In particular, the temperature, the applied pressure profile, and the amount of water present in the starting material[23]. The principle of the solid-solid transition is the thermal reflow, a phenomenon that allows the molecules to rearrange under a mechanical when the temperature is higher than the glass transition temperature (T_g). The presence of water act as a plasticizer reducing T_g and allowing an effective process even at low temperatures, down to 40 °C[23]. This method has been adopted to produce object in one step by compressing the starting material into a mold[26]. This resin was proved to reach compression modulus in the order of a gigapascal, however when tested after a prolonged period in a pseudo physiological condition their mechanical resistance dramatically dropped. A chemical crosslinking was obtained by the addition of Genipin to fibroin prior to the compression[27]. The crosslinking reaction triggered by the increase in temperature and the presence of water allowed to obtain a chemically crosslinked resin with a compression modulus high enough to be used in structural applications even in wet environments as the biological one[27].

The main disadvantage of all the previous protocols is the lack of porosity that does not allows to this resin to be applied as a structural scaffold. In this work we propose a modified compression molding protocol that allows to contemporary crosslink the silk fibroin and obtain a porous structure. The addition of citric acid (CA) in powder ensured both this effect, the fraction dissolved allows the crosslinking reaction while the other fraction acts as a pores template. CA has been previously used to crosslink starch[28], cellulose[29,30], chitosan[31], alginate[31,32], alginate[33], agarose[34], collagen[35] and gelatin[36]. In case of silk, CA has been previously used on the raw fibers[37] and in several cases as degumming agent to remove the external layer of sericin[38,39]. However, the crosslinking effect of CA on proteins was proved to occurs at relatively mild conditions low temperature in presence oh humidity) and to act on the amine side groups[40].

The resin produced was proved to be porous by SEM imaging and image analysis, and the effect of the crosslinking to be dependent to the amount of CA added. The resins have been mechanically tested by compression and crosslinking reaction, as well as the relative amount of secondary structures were evaluated by Fourier transform infrared spectroscopy (FTIR). To our knowledge this is the first attempt to use CA as crosslinking agent for silk fibroin and the first porous structural material produced with silk. A further complete biological evaluation will be needed to ensure the usability of this material for biomedical purposes.

2. Materials and Methods

2.1. Regenerated silk fibroin preparation

The degumming process was done following a procedure previously described[41,42] and shown in Figure 1A. Briefly, delaminated silk cocoons were placed in a bath of Na_2CO_3 aqueous solution, with a ratio 1.1 g of salt every liter of deionized water, at 98 °C for 90 minutes. In each degumming procedure, an amount of delaminated silk between 20 g and 30 g in weight was used (10g per liter of solution). Then to ensure the complete dissolution of sericin, the resulting silk was placed in a second bath of 0.4 g of Na_2CO_3 every liter of deionized water, at 98 °C for 90 minutes and

Preprints (www.preprints.org) | NOT PEER-REVIEWED | Posted: 4 January 2023 doi:10.20944/preprints202301.0058.v1

under stirring. After this step, different bath in deionized water at decreasing temperature were done, trying to maintain the following steps of bath temperatures: 80 °C, 65 °C, 50 °C 35 °C and then a final bath at room temperature. The degummed silk fibroin fibers were then manually squeeze and manually separated, to remove any entangled parts. Finally, the material was wrapped in a double layer of paper and dried under the hood for at least 48 hours. To ensure the complete sericin removal the weight loss was checked to be between 25 % and 30 % as established by previous works[41,42].

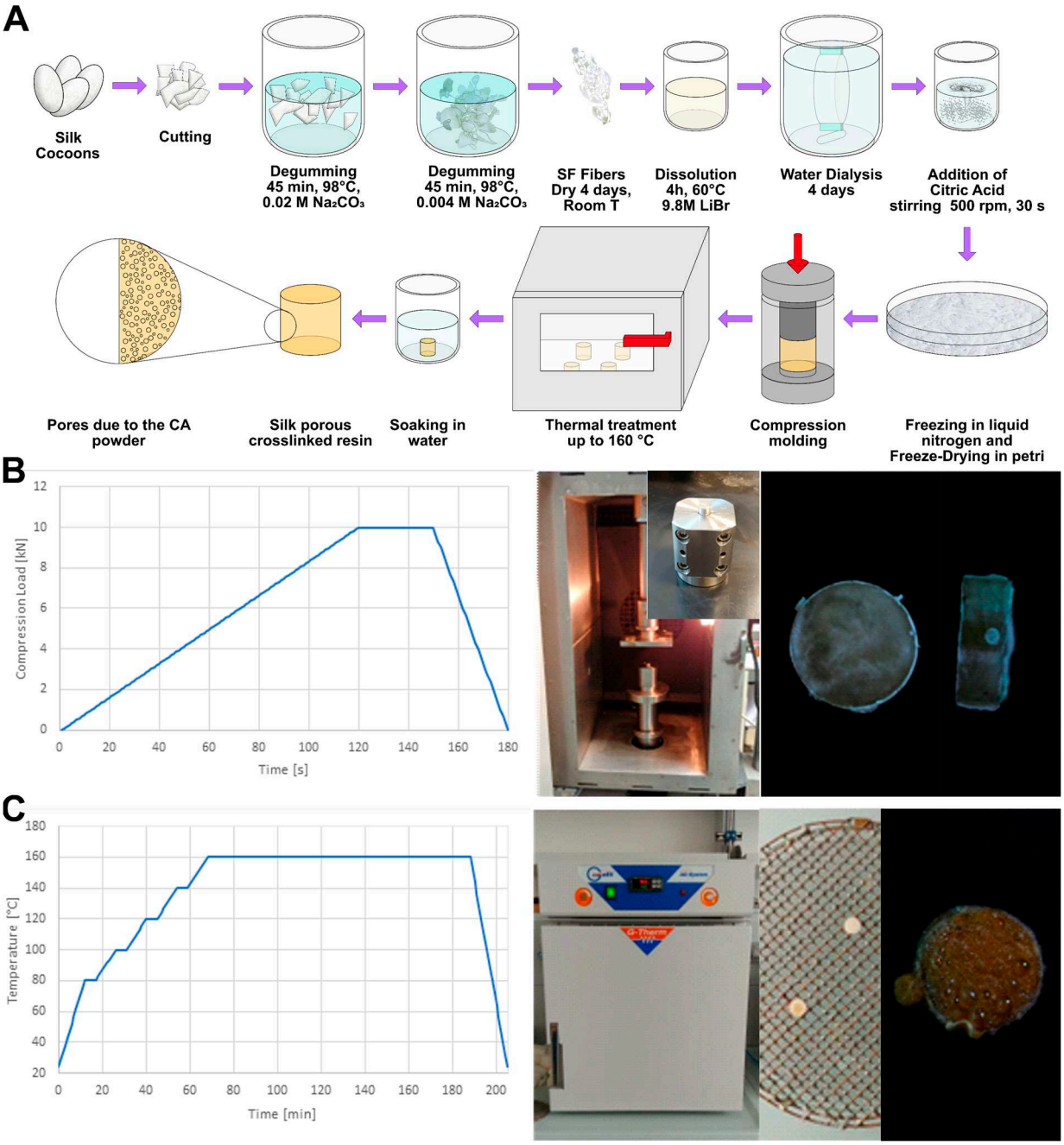

Figure 1. (**A**) Complete scheme of preparation. Briefly the cocoons were cut and degummed by two Na_2CO_3 baths at different concentrations, the degummed fibers were then dissolved in a LiBr solution. The resulting denaturated fibroin solution was dialyzed to remove the salt. Based on the concentration of fibroin in solution a calculated amount of citric acid was added and rapidly mixed. The solution was then frozen in liquid nitrogen and freeze-dried to produce a sponge. The sponge was compressed in a mold at a determined temperature. The compression molded fibroin resin was then thermally treated to allow the fusion of CA and then placed in water to remove its presence. The resulting object was porous. (**B**) Compression phase. The compression was done following a ramp, reaching 10kN in 120 s, holding the pressure for 30 s and releasing it in 30 s. The compression was

 doi:10.20944/preprints202301.0058.v1

done in a universal testing machine with ad oven that ensure the possibility to maintain a constant temperature. The mold was specifically designed to easily extract the compressed samples. An example of a prepared sample is shown in figure. (**C**) The thermal treatment was conducted in an oven following the reported temperature ramp up to 160 °C to allow the fusion of CA and its release. The samples were placed on a grinder, to let the fused CA dripping. The sample after thermal treatment resulted to be wet confirming the effectiveness of the procedure.

The degummed silk fibroin was placed in a solution of LiBr 9.3 M with a ratio 20 % w/v placed in an oven (Binder, E028-230V-T) at 65 °C for 4 hours, until complete dissolution. To remove the salt, the solution was dialyzed against deionized water using standard regenerated cellulose dialysis tubes (Spectra/Por, cutoff 3.4, 45 mm width), for 4 days. The resulting water solution was filtered to remove impurities and then checked in terms of pH and concentration. This last was determined by spectroscopic method (nanodrop 1000, ThermoFisher), by verifying the absorbance of the solution at 280 nm and using the internal calibration of the instrument to determine the mg of fibroin for each mL.

2.2. Silk fibroin sponges

Knowing fibroin concentration in the dialyzed solution, typically around 40 mg/ml, the right amount of citric acid (CA) was added. Different concentrations of CA were selected based on the processability of the final compound and on the aim to obtain an efficient crosslinking and pores formation. The objective was to add enough citric acid to show enhancement in mechanical properties given by crosslinking effect and to leave a variable porosity based directly on the amount of citric acid added, with a further process of heat treatment, later described. Three main concentrations of citric acid were chosen based on a preliminary evaluation that took into consideration a wide range of CA concentrations (from 0.25 to 2 in weight ratio CA/SF). Based the weight of SF we added CA in a ratio of 0.25, 0.50 or 0.75 (CA/SF w/w). Then to remove completely the water we performed a freeze drying. Briefly the samples were soaked in liquid nitrogen for 15 minutes to allows their freezing and then placed in a Freeze-drier (Lio 5P, 5Pascal) and freeze dried at -45 °C for days. As result a sponge was obtained Due to the presence of CA the samples were lyophilized in large petri dish to increase the surface and speed up the process. After freeze drying the samples were stored in a dryer until their use.

2.3. Thermoplastic molding

To produce the bulk resin the freeze-dried material was compressed using a universal testing machine (858 Mini Bionix, MTS) as schematized in Figure 1A with an oven that allowed to set the temperature. The applied compression ramp is shown in Figure 1B. The compression cycle to produce bulk samples consisted in a ramping load of 120 s until the maximum load value of 10 kN, a steady period of 30 s and a finale discharge of 20 s until zero load. Compression was carried out in a plate-plate configuration, using a demountable mold, to facilitate the removal of the specimen. Each sample was prepared starting from 200 mg of spongy material. Three different temperatures in sintering process were used to study the activation of crosslinking behavior of citric acid on silk fibroin: 40 °C, 80 °C and 120 °C. The maximum limit of temperature of 120 °C was selected because of the difficulty in compression at higher temperatures, which led to a compound with low viscosity, resulting in a material flow through mold slit. The metallic mold was introduced in the MTS furnace, set to the desired temperature and at least two hours was waited to bring the mold at the right temperature. Because of the time needed to charge mold with the lyophilized material, and being this step done outside the oven, at room temperature, after every cycle of compression, a 5 minutes of heating step was considered to compensate the cooling down of the mold and to have a stable sintering temperature for each specimen.

 doi:10.20944/preprints202301.0058.v1

2.4. Thermal treatment

To attempt in obtaining porosity on the surface and inside the bulk silk fibroin component, a degradation of citric acid was made. This concept took advantage of the presence of large amount of citric acid entrapped in the fibroin structure and the capability of thermally release it. From literature, the initial degradation temperature of citric acid is reported as 153 °C and for this reason a heating of the sintered material in an oven G-Therm (Fratelli Galli) up to 160 °C following the temperature ramp described in **Figure 1C**. The temperature was maintained for 5 minutes at each thermal step, considering steading temperatures fixed on 80 °C, 100 °C, 120 °C, 140 °C and finally the operative temperature of 160 °C. Samples were placed on a metallic grill over a glass petri dish, to allow even the release of citric acid below specimens.

After this heating step, for some samples it was even possible to observe melted citric acid on the surface. In order to improve the removing of this melted citric acid and to allow porosity formation, the samples were soaked in a bath in deionized water. The bath step consisted in the immersion of heated samples in a beaker containing 100 ml of deionized water for 10 minutes. At the end of the process, samples were stored in vacuum for at least 48 hours to allow the complete dehydration.

2.5. Morphological Analysis

Field-Emission Scanning Electron Microscopy (FE-SEM Supra 60, Carl Zeiss) analysis was done on fracture surface of samples. To produce a fragile breakage, specimens were wrapped in aluminum foil and then immersed in liquid nitrogen for 3 minutes. Frozen specimens were then hit by a chisel using a hammer with a precise and rapid strike. Fragments of samples were stored in vacuum for 24 hours, to be sure in removing any trace of humidity. The cross-section surfaces were metallized by sputtering with a thin Pl/Pd layer. Micrography pictures were analyzed by FIJI software (National Institute of Health, v.1.53t), to obtain a direct result on pore size distribution by a segmentation with thresholding.

2.6. Mechanical Analysis

Mechanical analysis was done in a pseudo-physiological condition and in compression with a universal testing machine (Instron 4502, Instron). For each sample, three replicas were prepared and tested in wet conditions to mimic the real application state. This testing condition was obtained by immersion of heat-treated samples in deionized water for 5 minutes or directly using samples after salt leaching process. Each specimen was measured in diameter and width by a caliber, to obtain precise data on stress and strain results, further calculated. Samples were then mechanically tested with a plate-to-plate configuration (Figure 2.14) using a 10 kN load cell, with an interlock for maximum load set on 9.5 kN. Compression test was made at a displacement rate of 1 mm/min as a standard parameter and test was carried out until breakage of sample or at least 1.5 mm of displacement, considering the material in a plastic deformation field.

Mechanical properties were then analyzed comparing the three main samples with different citric acid ratio: 0.25 CA/SF (w/w), 0.5 CA/SF (w/w) and 0.75 CA/SF (w/w). Also, the study of the effect of sintering temperature on material elastic modulus was carried out. Finally, a relation between mechanical properties and pores dimensions and interconnections was considered.

Preprints (www.preprints.org) | NOT PEER-REVIEWED | Posted: 4 January 2023 doi:10.20944/preprints202301.0058.v1

2.7. Fourier Transform Infrared (FTIR) Analysis

Considering the secondary structure of silk fibroin as a protein, and its variations due to the crosslinking effect, a direct study on the secondary structure of the amine group of this protein was made. This study was done on samples with different concentration of citric acid, to observe the eventual variation of secondary structure responsible of crosslinking phenomenon, in particular the β-sheet structure.

Every sample was dried in vacuum for 24 hours before to be tested with FTIR. The important evaluation was the study of the fundamental peaks, in particular the primary and secondary amide peaks respectively with center at 1620 cm^{-1} and 1538 cm^{-1}. The infrared analysis was done in total attenuated reflectance (ATR) mode (Spectrum ONE, Perkin Elmer) measuring the transmittance spectra as mean of 16 scans in the range of primary amide 1590-1720 cm^{-1} with a resolution of 1 cm^{-1}.

The analysis was performed as previously descripted[42,43]. The primary amide peak was smoothed and then a Fourier self-deconvolution was applied (smoothing factor 0.3, gamma function 30). This allowed to obtain well defined peaks for each secondary structure contribution. Peaks position was found by a second derivative. Then the peaks were fitted by a Gaussian function, imposing the minimization of χ^2. The assignment of the structure was done following Table 1. The area of each pack was calculated and divided by the total area (sum of the peaks area) to determine the relative percentage amount of the considered secondary structure.

Table 1. Peaks assignment for the quantification of the percentage of secondary structures.

Secondary Structure	Wavenumber range [cm^{-1}]
Side chain	1597-1609
β-sheets	1610-1625
β-sheets	1626-1635
Random coils	1636-1655
α-helix	1656-1662
β-turns	1663-1696
β-sheets	1697-1703

3. Results

3.1. Citric Acid addition and liophilization

As previously described, citric acid was added to obtain a crosslinking of the material and to obtain a certain degree of porosity. The addition of citric acid created some difficulties in the production steps of the standard process already established from our previous works[23,27]. The initial trials were conducted with an excess of citric acid compared to the weight of the regenerated silk a wide range of CA/SF ratio, ranging from 1 CA/SF to 4 CA/SF (as shown in Figure 2A, normal).

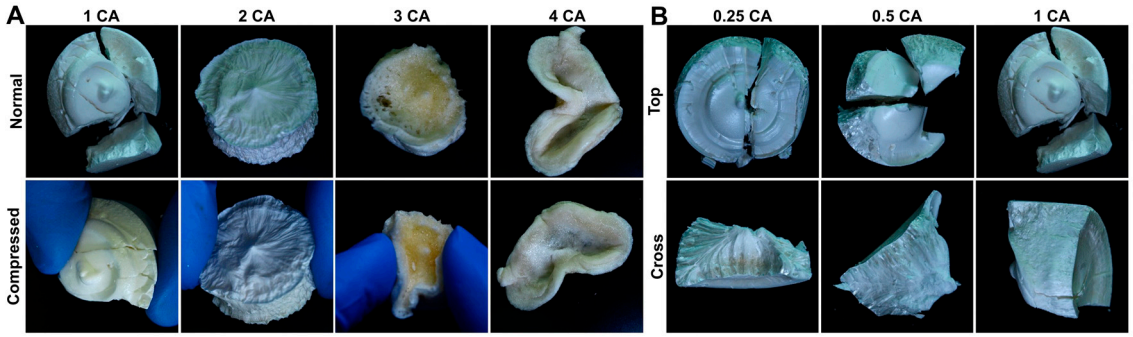

 doi:10.20944/preprints202301.0058.v1

Figure 2. (**A**) Sponges with addition of citric acid (CA) with a CA/SF ratio (w/w) ranging from 1 to 4. Only the sample with the lower amount of CA was completely lyophilized. The samples resulted to be less deformable under manual compression with the increasing of CA up to 2 CA/SF, above the hygroscopicity of the salt made the freeze drying not feasible. It should be noticed that also the core of the 2 CA/SF sample resulted to be still not dry. (**B**). The sample used for the compression molding were produced with ratios ranging from 0.25 to 0.75. This last was chose as the upper limit from the initial evaluation.

After lyophilization step of the freeze-drying process, an initial increase of the hardness was observed with the increase of CA content, but above 2 CA/SF the incomplete freeze-drying gave soft samples, clearly visible when a pressure was manually applied (Figure 2A, compressed). It should be noticed that the sample with the higher amount of CA (4 CA/SF) was so soft that it was deformed in during the extraction from the mold. This was attributed to the hygroscopic property of citric acid and the consequent water retention in the sponge structure, even after lyophilization. Nevertheless, even in the case of 2 CA/SF, the external rigid appearance contained a soft core, with a high amount of retained water. This was a symptom of a non-well lyophilized material. 1 CA/SF was the sole to be completely lyophilized and, for this reason, it was considered as the maximum limit value of citric acid concentration for freeze-drying optimal process. Imposing this limit, the new citric acid concentration considered for further production steps were set to 0.25 CA/SF, 0.5 CA/SF and 1 CA/SF, for which the aspect was of a sponge-like material, as observed from the fracture surface (Figure 2B, cross).

3.2. Compression molding

Despite freeze-drying process results, samples with high citric acid concentration were sintered, to observe the effect of the natural crosslinker on the final bulk product. CA/SF ratios between 0.25 and 2 were evaluated, to analyze the further possibility of pores formation with citric acid degradation. Sintering process was done at 4 different temperatures: Room Temperature (RT), 40 °C, 80 °C and 120 °C. The increasing temperature was considered to allow and improve the crosslinking capability of citric acid. In Figure 3A the produced samples are shown.

From the sintering process, it was possible to observe the typical change in colour of fibroin, with increasing sintering temperature, from shiny white to transparent yellowish. The main problem in the use of citric acid during the sample production process was to reduce the viscosity of the material inside the mold, during sintering step. The combining action of increasing the temperature and citric acid concentration led to the reduction of viscosity of the sintering material, with the loss of the cylindrical shape during compression, this resulted in the failure of the compression step. This problem was encountered for samples with citric acid ratio higher than 1 CA/SF.

Preprints (www.preprints.org) | NOT PEER-REVIEWED | Posted: 4 January 2023 doi:10.20944/preprints202301.0058.v1

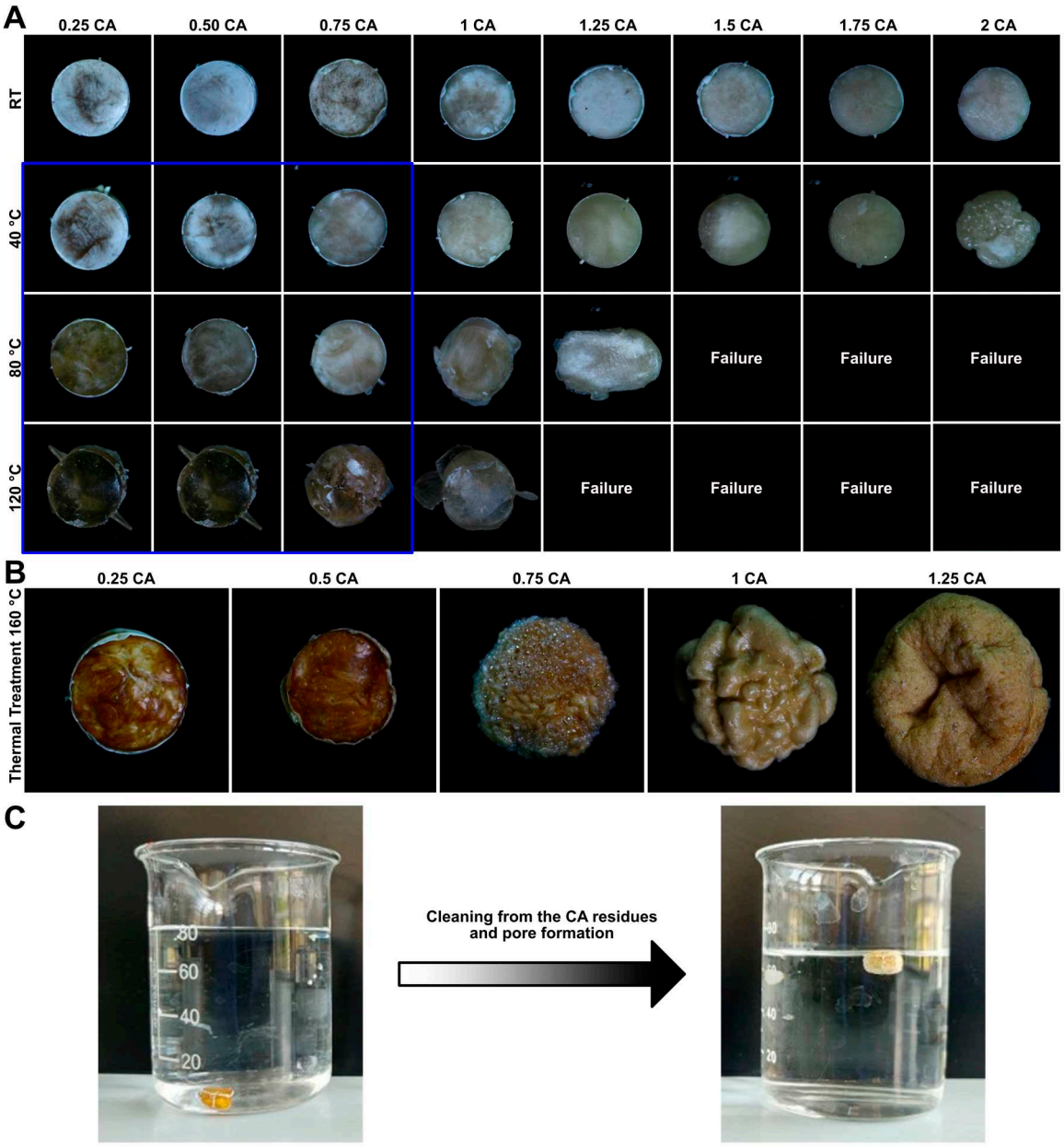

Figure 3. (**A**) Fibroin samples from the compression molding step. The samples indicated with failure were completely deformed during the compression. The shape was acceptable in a wide range of conditions. However, we decided to test only the samples that did not lose their shape during the following thermal treatment and to exclude the samples produced at room temperature (RT) that did not ensure an effective solid-solid transition. The tested samples are enclosed in the blue rectangle. (**B**) Thermal treatment (up to 160°C) of samples produced with a compression molding at 80 °C. Samples with a CA equal or above 1 CA/SF dramatically changed their shape. For this reason, only samples with lower amount of CA were tested in the following phases. (**C**) Step of CA removal in deionized water. Samples started to float as effect of the CA removal.

As shown in Figure 3A, 1 CA/SF sample gave a low reliability in the final shape of molded bulk materials for sintering temperatures higher than 40 °C. Samples compressed at RT resulted to be difficult to control in terms of material converted to resin, they were excluded from the following phases.

Preprints (www.preprints.org) | NOT PEER-REVIEWED | Posted: 4 January 2023 doi:10.20944/preprints202301.0058.v1

3.3. Thermal tretment

After sintering process, to make the sample porous a thermal treatment was done. Samples were heated throught a temperature ramp up to 160 °C to degrade citric acid, which was removed with a deionized water bath, in order to leave pores behind. A set of thermally treated samples are reported in Figure 3B. These samples were produced with a compression molding at 80 °C and an increasing amount of CA. A strong deformation of the samples was observed above 0.75 CA. This phenomenon was attributed to the strong kinetic in citric acid release from the core of the molded cylinder. Samples with a CA ratio contentment above 0.75 were not further tested.

During the immersion in water the samples started to float (Figure 3C) as a result of the progressive cleaning from the residual CA. This was a poof of the formation of the pores and the decreasing in the sample density.

3.4. Morphological Analysis

Samples were broken to reveal the internal surface and analyze the pore distribution. The SEM micrographies are shown in Figure 4A while the comparison between the pore distributions in the box plots of Figure 4B. Regarding 0.25 CA/SF samples, increasement of sintering temperature didn't lead to an evident variation in pore structure (as clearly visible from the micrographies). Fracture surface was characterized always by not-interconnected pores and only in few sites, of the sample compressed at 40 °C, some interconnection of pores was found. The general structure for 0.25 CA/SF was characterized by a non-homogenous distribution of pores with a wide range in size. In addition, by the analysis of pores distribution, the mean equivalent diameter measured for each sintering temperature of 0.25 CA/SF sample was always below 5 μm and increasing the sintering temperature a wider distribution of values was obtained, if compared with the sharp diameter distribution of 40 °C in sintering.

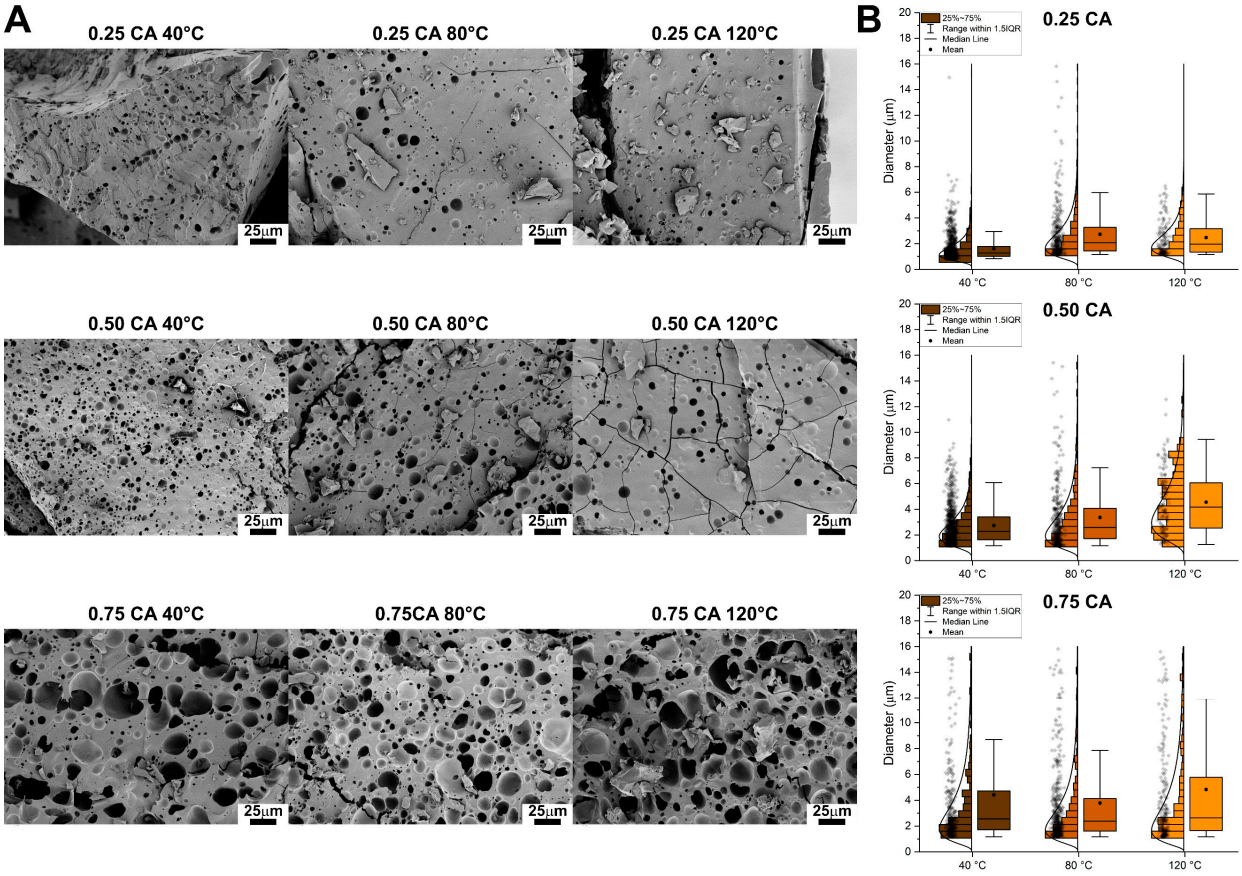

Figure 4. (**A**) SEM images collected from the cross section of the samples. How can be observed the increase in the amount of CA increase the porosity while the effect of the temperature was not so

Preprints (www.preprints.org) | NOT PEER-REVIEWED | Posted: 4 January 2023 doi:10.20944/preprints202301.0058.v1

pronounced. (**B**) Box plot comparing the pore diameter distributions with different CA/SF ratio obtained at different temperatures but the same CA/SF ratio. The box plots are reported with the datapoints, the distribution histogram and the log-normal distribution used to fit them.

Regarding 0.5 CA/SF samples, an apparent increase of porosity is obtained respect to 0.25 CA/SF sample and in particular for 40 °C pores start to show an interconnected structure. Increasing the sintering temperature to 80 °C and 120 °C this interconnection is apparently loss and for this last temperature the pores were not interconnected. For both 0.25 CA/SF and 0.5 CA/SF samples the microstructure obtained by compression molding at 120 °C was characterized by small, isolated pores, explained the higher mechanical properties showed in the previous analysis. For this reason, the sintering temperature of 120 °C was considered inconvenient for the production process adopted. The quantitative analysis showed mean values of pores diameters lower than 5 μm, but with a large distribution reaching higher values, even until 10μm.

Analyzing micrographs for sample 0.75 CA/SF, pores appeared larger and better interconnected than previous samples. This enhancement of porosity results could explain the lower mechanical properties and despite the higher interconnection, this citric acid concentration was difficult to be considered valid for material production. From the quantitative consideration, 0.75 CA/SF showed, for each sintering temperature, a further increase in the overall pore's dimensions, reaching higher mean values and the presence of 15 μm pores in diameter.

3.5. Mechanical Analysis

Citric acid crosslinked samples showed a visible compact structure considering the three main CA/SF ratios. Swelled samples were not measured by mechanical test, because their deterioration even with simply manually treatment.

Samples were analyzed after thermal treatment and for all the three sintering temperatures used. It is important also to consider that every sample was tested in wet conditions, in order to mimic the final application conditions of the material. The mechanical tests were obtained in compression and load-displacement results were reported. Therefore, by the measure of specimens' cylindrical dimensions, stress-strain curves were plotted, and elastic modulus was calculated as a mechanical properties reference.

A general observation of the results shows the progressive increase of load with the displacement, and then increase of stress with the material strain, and this is due to the continuous compaction of the material and the closure of the pores, initially present. Therefore, tests were carried out with advanced deformation of the samples, in order to show this permanent collapse of pores. The initial part of curves was interesting to extrapolate the elastic modulus, considering the characteristic behaviour obtained before pores closure.

Table 2. Descriptive statistic of the pore diameter distributions. All of them resulted to be skewed to the lower values, however with the increasing of the CA amount the distribution become wider (IQR increases).

CA/SF	T	Mean	StD	Skew	Kurt	Min	Q1	Median	Q3	Max	IQR
w/w	°C	μm	μm	μm	μm	μm	μm	μm	μm	μm	μm
0.25	40	2.47	1.37	1.17	0.49	1.17	1.35	1.96	3.16	6.51	1.81
0.25	80	2.73	2.08	2.95	11.64	1.17	1.43	2.08	3.27	15.81	1.84
0.25	120	1.62	1.07	3.75	29.06	0.83	1.01	1.26	1.78	14.95	0.77
0.50	40	2.74	1.54	1.57	2.62	1.17	1.62	2.27	3.40	10.97	1.79
0.50	80	3.37	2.52	2.36	7.14	1.17	1.72	2.59	4.07	17.29	2.35
0.50	120	4.56	2.34	0.68	0.10	1.26	2.54	4.17	6.06	12.56	3.52
0.75	40	4.43	4.64	2.43	5.91	1.17	1.72	2.55	4.73	26.39	3.01
0.75	80	3.79	3.71	2.63	7.75	1.17	1.62	2.38	4.13	22.69	2.51

Preprints (www.preprints.org) | NOT PEER-REVIEWED | Posted: 4 January 2023 doi:10.20944/preprints202301.0058.v1

0.75	120	4.83	4.93	2.12	5.07	1.17	1.65	2.63	5.78	30.29	4.13

For 0.25 CA/SF samples, increasing the sintering temperature, no relevant effects were observed on the final mechanical properties, regarding the stress-strain curves (Figure 5A). In general, for all curves, an initial flat tract was considered as settlement of the higher punch to the specimen surface. Samples were broken with a fragile behaviour, with the formation of small debris, like powder. This brittleness was given by the thermal treatment and confirmed during the specimen cutting for SEM analysis. For all samples, after 1 mm of displacement the formation of debris was already visible and compaction stress started to increase.

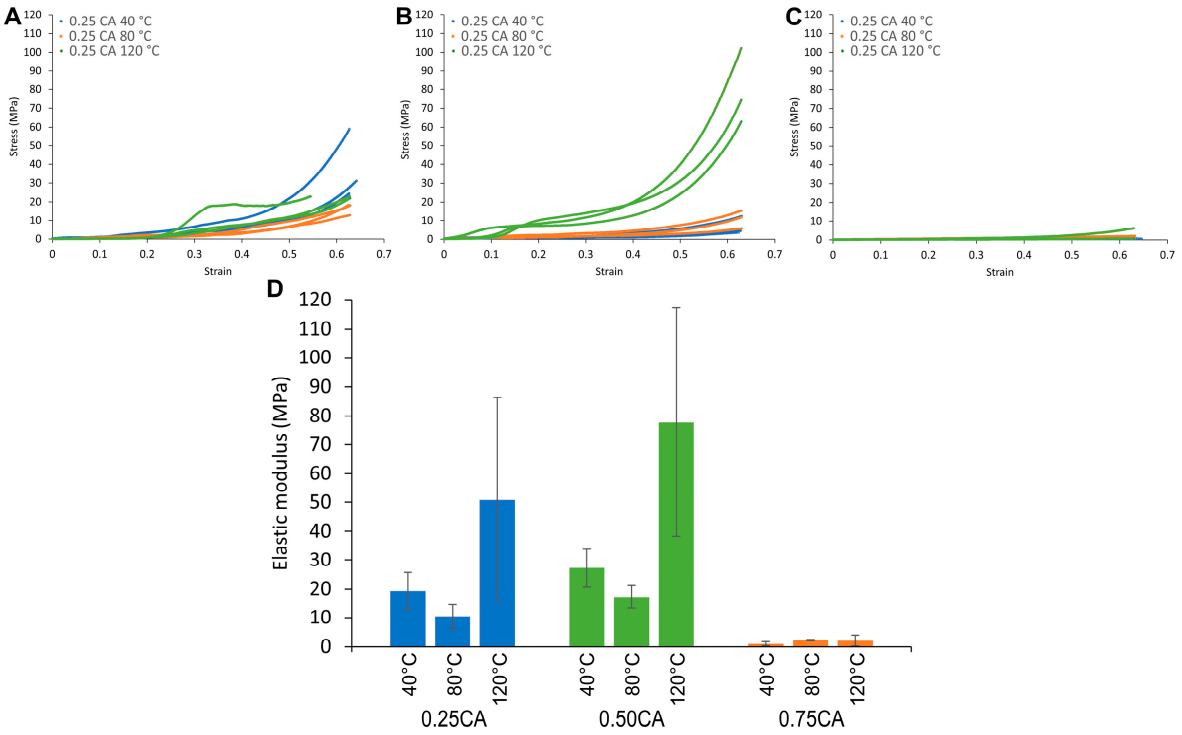

Figure 5. Stress-strain curves for samples compressed at different temperatures with the CA/SF ratios of (**A**) 0.25 (**B**) 0.50 and (**C**) 0.75. All the samples were tested in a pseudo-physiologic condition (after water soaking at 37 °C. (**D**) Summary results in term of compression modulus. An increment of the compression modulus was recorded by the increment in CA/SF ratio from 0.25 to 0.50 however a further increment in CA (CA/SF 0.75) content strongly decreased the compression modulus.

For 0.5 CA/SF samples, the results were similar as previous sample, with a general increase in mechanical properties for 120 °C of sintering temperature (Figure 5B). It was attributed to the higher amount of citric acid, able to enhance the mechanical properties of the previous sample. For 0.75 CA/SF stress values are strongly reduced and the bulk sintered material is not able to sustain the load after thermal treatment (Figure 5C). This process was creating a too fragile material for higher content of citric acid and this sample was not considered reliable for the production of a porous scaffold. To consider a quantitative measure of mechanical properties for these samples, the first part of the stress-strain curve was considered for the measure of the elastic modulus. In this tract of the curve, the material was elastically deformed, and no debris was formed. As already described, also an initial settlement of the system was considered, to not also measure the initial displacement of the Instron punch until material touching. For each sample, increasing the sintering temperature, there was not a continuous trend in the variation of the elastic modulus (Figure 5D). The higher value was obtained with 120 °C of sintering temperature, but with a low reliability in terms of absolute value. Sintering at 40 °C showed a higher elastic modulus respect to 80 °C, and for both, the results were more reliable in different specimens.

 doi:10.20944/preprints202301.0058.v1

In addition, moving from 0.25 CA/SF to 0.5 CA/SF, elastic modulus was increased for each sintering temperature used, but further increasement of citric acid (to 0.75 CA/SF), the elastic modulus brutally decreased, as expected also by the trend of the stress-strain curves. For this reason, the excess of citric acid, to obtain higher porosity with thermal treatment, was neglected as solution.

The overall consideration of mechanical properties in terms of stress values was in the order of 10-20 MPa as mechanical strength, before the formation of debris and the compaction of the formed powder. These low mechanical properties were attributed to the thermal treatment, which led the material to a brittle behaviour. Therefore, in order to increase the mechanical properties, this treatment was substituted, and porosity was formed by salt leaching in the advanced samples, further described. In addition, silk microfibers were added to the silk fibroin solution, to incorporate microfibers in the general structure and to increase the capability in sustain loads.

3.6. Structural Analysis

In Figure 6A the spectra of compressed molded silk fibroin (SF-CM), compressed molded silk fibroin with the addition of citric acid (SF_0.50CA-CM) and citric acid (CA), are reported. All the samples were produced by compression molding at 80 ◦C. In the SF spectra the peaks centered around 1617 cm^{-1}, 1510 cm^{-1} and 1225 cm^{-1} were assigned to the Amide I, Amide II and Amide III, respectively. The two peaks detectable in CA at 1751 cm^{-1} and1507 cm^{-1} indicates the C=O stretching of carboxylic acid. Those peaks disappeared in the SF_0.50CA_CM spectra where a peak appeared at 1700 cm^{-1} indicating of the presence of carbonyl groups, which confirmed the protein crosslinking, as previously revealed in literature. Interestingly, the increment in the CA content produced an increase in the 1700 cm^{-1} peak, as highlighted by the arrow in Figure 6B indicating an increase in the crosslinking degree.

The Amide II peak was further deconvolved to reveal the different percentage of secondary structures before (Figure 6C) and after (Figure 6D) thermal treatment and compared to a sample prepared by compression molding of silk fibroin (SF-CS) at 80◦C. The addition of CA generally increased the percentage amount of the crystalline β- phase at the expenses of the random coil phase.

Preprints (www.preprints.org) | NOT PEER-REVIEWED | Posted: 4 January 2023 doi:10.20944/preprints202301.0058.v1

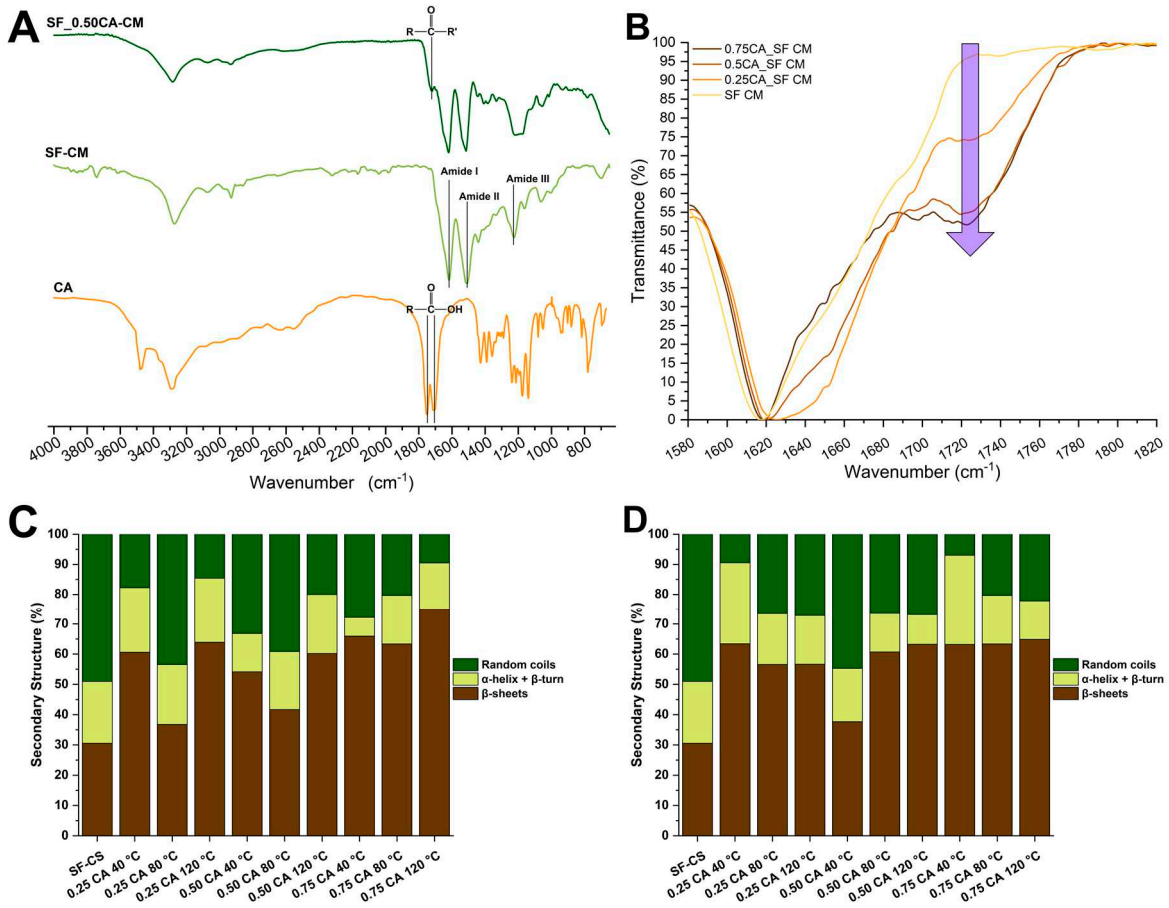

Figure 6. (**A**) FTIR spectra of citric acid (CA), a sample obtained by compression molding of lyophilized silk fibroin (SF-CA) and a sample in which CA was added prior to compression molding (SF_0.50CA-CM). by comparing the spectra, it was possible to spot the formation of a peak indicating the presence of carboxyl groups when CA was added to fibroin which confirm the protein crosslinking. (**B**) The intensity of carboxyl peak increased with the increasing in the CA amount indicating a higher degree of crosslinking. (**C**) Relative amount in percentage of secondary structures before the thermal treatment. (**D**) Relative amount in percentage of secondary structures after the thermal treatment. The presence of CA increased the crystalline structure compared to the compressed sample without CA (SF-CS). A small effect of the thermal treatment on the relative percentage was detected.

The increase in temperature from 40°C to 80°C decreased the effectiveness in the transition to β, while the increase to 120◦C was the more effective treatment. The higher amount of crystalline structures was obtained by the compressions at 120°C. After the thermal treatment (Figure 6B) the trend became less clear, this may be due to the complex effect of the CA decomposition and the contemporary trigger of the high temperature towards the fibroin crystallization.

4. Discussion

In this work we studied the production of a silk resin by thermoplastic molding in which the addition of CA ensured both the formation of a porous structure and the crosslinking of the protein chains. The crosslinking effect on proteins was previously studied and was Only a subset of the produced samples was chosen to indagate their properties. In this subset the samples were sufficiently converted from the sponge to the resin, and they were not completely deformed by the thermal treatment. This included three CA/SF ratio 0.25, 0.5, and 0.75.

From the microstructural point of view all while all previous developed protocols were unable to generate a porosity[19–24,27], the addition of CA was effective in generating pores which mean dimeter was related to the amount of CA added. Higher the amount of CA higher the mean diameter

and higher the number of pores generated. The higher amount of CA added (0.75 CA/SF) gave a structure that resemble a sponge but with thicker walls. It should be noticed that the porosity generated by our method was far from the porosity obtained with other methods (like freeze-drying, foaming and others) specifically developed to obtain a spongy SF architecture[9–16]. In fact, SF sponges usually have a wide pores dimensional distribution with diameters that reaches hundreds of micrometers while in our case we were able to obtain pores with diameters of tens of micrometers. However, this is to our knowledge the first successful attempt to produce a structural porous biopolymeric material.

The crosslinking effect was detected by the increase in the compression modulus moving from 0.25 CA/SF to 0.5 CA/SF while a further increase to 0.75 CA/SF ratio. This could be explained by the structural analysis, in fact, the increase to 0.75 CA/SF gave a particularly porous structure which was probably less resistant to the load bearing. Compared to the fully compact resins obtained in previous works the compression modulus of our most performant sample was similar to the modulus obtained in pseudo-physiological condition in case of crosslinking with genipin[27] and higher than the modulus tested in wet conditions in not crosslinked SF resins [23,26]. This further confirmed the effect of CA in crosslinking the SF chains.

The crosslinking was confirmed also by the FTIR analysis in which the peak related to the presence of carbonyl groups, which intensity increased with the increasing in CA content. It should be noticed that this increase was almost linear moving form 0 CA/SF, 0.25 CA/SF to 0.50 CA/SF but it reached a sort of plateau moving from 0.50 to 0.75. This may indicate that a complete crosslinking was reached at ratios below 0.75 CA/SF. The addition of CA increased the relative percentage amount of β-sheets compared to the sample produced without CA. This effect was similar to one obtained by dissolution of Silk in formic acid the simpler organic acid and could be explained by the same mechanism, an interaction triggered by the presence of polar groups in both CA and SF that led to compact the SF molecules and generate intramolecular H-bonds [44–46].

In this work we did not perform any biological evaluation, because of the wide literature present for both SF and CA the sole two materials used in this study. However, in a follow-up study we will investigate the biological performances of this material by *in-vitro* screening.

5. Conclusions

The use of silk resins obtained by compression molding is generally not suitable for scaffolding due to the internal microstructure that is compact and non-porous. In this work by the addition of citric acid to the thermoplastic molding of silk achieved two purposes: produce a porosity inside to the compact structure and chemically crosslink the SF chain. This material had a compression modulus comparable to a previously developed crosslinked SF resin with the addition of a porosity that makes it suitable for scaffolding purposes. The FTIR was used to confirm the effective crosslinking. The best sample in terms of mechanical performances was obtained by compression at 120◦C with a CA/SF ratio of 0.50. This material may be used in the future as a structural bone scaffold made of SF a known bioresorbable biopolymer. A further complete biological evaluation will be needed to understand the interaction of this material with the biological tissues and verify its usability as biomedical device.

Author Contributions: Conceptualization, A.B, N.V., and D.M; methodology, A.B, N.V. and D.M.; formal analysis, A.B. and N.V.; investigation, N.V.; data curation, A.B.; writing—original draft preparation, A.B.; writing—review and editing, A.B., A.M.B., B.G. and D.M.; visualization, A.B.; supervision, A.M., B.G., and D.M.; project administration, D.M.; funding acquisition, D.M., and B.G. All authors have read and agreed to the published version of the manuscript.

Data Availability Statement: Data is available from the authors upon reasonable request.

Acknowledgments: This work was supported by IRCCS Istituto Ortopedico Rizzoli (Ricerca Corrente).

Conflicts of Interest: The authors declare no conflict of interest.

References

1. Bucciarelli: A.; Motta, A. Use of Bombyx mori silk fibroin in tissue engineering: From cocoons to medical devices, challenges, and future perspectives. *Biomater. Adv.* **2022**, *139*, 212982, doi:10.1016/j.bioadv.2022.212982.
2. Kundu, B.; Rajkhowa, R.; Kundu, S.C.; Wang, X. Silk fibroin biomaterials for tissue regenerations. *Adv. Drug Deliv. Rev.* **2013**, *65*, 457–470, doi:10.1016/j.addr.2012.09.043.
3. Cheng, G.; Wang, X.; Tao, S.; Xia, J.; Xu, S. Differences in regenerated silk fibroin prepared with different solvent systems: From structures to conformational changes. *J. Appl. Polym. Sci.* **2015**, *132*, n/a-n/a, doi:10.1002/app.41959.
4. Holland, C.; Numata, K.; Rnjak-Kovacina, J.; Seib, F.P. The Biomedical Use of Silk: Past, Present, Future. *Adv. Healthc. Mater.* **2019**, *8*, 1800465, doi:10.1002/adhm.201800465.
5. Raggio, R.; Bonani, W.; Callone, E.; Dirè, S.; Gambari, L.; Grassi, F.; Motta, A. Silk Fibroin Porous Scaffolds Loaded with a Slow-Releasing Hydrogen Sulfide Agent (GYY4137) for Applications of Tissue Engineering. *ACS Biomater. Sci. Eng.* **2018**, doi:10.1021/acsbiomaterials.8b00212.
6. Yan, S.; Feng, L.; Zhu, Q.; Yang, W.; Lan, Y.; Li, D.; Liu, Y.; Xue, W.; Guo, R.; Wu, G. Controlled Release of BMP-2 from a Heparin-Conjugated Strontium-Substituted Nanohydroxyapatite/Silk Fibroin Scaffold for Bone Regeneration. *ACS Biomater. Sci. Eng.* **2018**, *4*, 3291–3303, doi:10.1021/acsbiomaterials.8b00459.
7. Melke, J.; Midha, S.; Ghosh, S.; Ito, K.; Hofmann, S. Silk fibroin as biomaterial for bone tissue engineering. *Acta Biomater.* 2016.
8. Bhattacharjee, P.; Kundu, B.; Naskar, D.; Kim, H.-W.H.-W.; Maiti, T.K.; Bhattacharya, D.; Kundu, S.C. Silk scaffolds in bone tissue engineering: An overview. *Acta Biomater.* **2017**, *63*, 1–17, doi:10.1016/j.actbio.2017.09.027.
9. Nazarov, R.; Jin, H.J.; Kaplan, D.L. Porous 3-D scaffolds from regenerated silk fibroin. *Biomacromolecules* **2004**, doi:10.1021/bm034327e.
10. Tamada, Y. New process to form a silk fibroin porous 3-D structure. *Biomacromolecules* **2005**, *6*, 3100–3106, doi:10.1021/bm050431f.
11. Mandal, B.B.; Kundu, S.C. Non-bioengineered silk fibroin protein 3D scaffolds for potential biotechnological and tissue engineering applications. *Macromol. Biosci.* **2008**, doi:10.1002/mabi.200800113.
12. Zhang, X.; Cao, C.; Ma, X.; Li, Y. Optimization of macroporous 3-D silk fibroin scaffolds by salt-leaching procedure in organic solvent-free conditions. *J. Mater. Sci. Mater. Med.* **2012**, doi:10.1007/s10856-011-4476-3.
13. Yao, D.; Dong, S.; Lu, Q.; Hu, X.; Kaplan, D.L.; Zhang, B.; Zhu, H. Salt-leached silk scaffolds with tunable mechanical properties. *Biomacromolecules* **2012**, doi:10.1021/bm301197h.
14. Bucciarelli, A.; Muthukumar, T.; Kim, J.S.; Kim, W.K.; Quaranta, A.; Maniglio, D.; Khang, G.; Motta, A. Preparation and Statistical Characterization of Tunable Porous Sponge Scaffolds using UV Cross-linking of Methacrylate-Modified Silk Fibroin. *ACS Biomater. Sci. Eng.* **2019**, *5*, 6374–6388, doi:10.1021/acsbiomaterials.9b00814.
15. Nam, Y.S.; Yoon, J.J.; Park, T.G. A novel fabrication method of macroporous biodegradable polymer scaffolds using gas foaming salt as a porogen additive. *J. Biomed. Mater. Res.* **2000**, doi:10.1002/(SICI)1097-4636(2000)53:1<1::AID-JBM1>3.0.CO;2-R.
16. Maniglio, D.; Bonani, W.; Migliaresi, C.; Motta, A. Silk fibroin porous scaffolds by N2O foaming. *J. Biomater. Sci. Polym. Ed.* **2018**, doi:10.1080/09205063.2018.1423811.
17. Luo, K.; Yang, Y.; Shao, Z. Physically Crosslinked Biocompatible Silk-Fibroin-Based Hydrogels with High Mechanical Performance. *Adv. Funct. Mater.* **2016**, *26*, 872–880, doi:10.1002/adfm.201503450.
18. Farokhi, M.; Aleemardani, M.; Solouk, A.; Mirzadeh, H.; Teuschl, A.H.; Redl, H. Crosslinking strategies for silk fibroin hydrogels: promising biomedical materials. *Biomed. Mater.* **2021**, *16*, 022004, doi:10.1088/1748-605X/abb615.
19. Tuan, H.A.; Hirai, S.; Tamada, Y.; Akioka, S. Preparation of silk resins by hot pressing Bombyx mori and Eri silk powders. *Mater. Sci. Eng. C* **2019**, *97*, 431–437, doi:10.1016/J.MSEC.2018.12.060.
20. Anh Tuan, H.; Hirai, S.; Inoue, S.; A. H. Mohammed, A.; Akioka, S.; Ngo Trinh, T. Fabrication of Silk Resin with High Bending Properties by Hot-Pressing and Subsequent Hot-Rolling. *Materials (Basel).* **2020**, *13*, 2716, doi:10.3390/ma13122716.
21. Tao, Y.; Xu, W.; Yan, Y.; Wu, H. Structure and properties of composites compression-molded from silk fibroin powder and waterborne polyurethane. *Polym. Adv. Technol.* **2012**, *23*, 639–644, doi:10.1002/pat.1938.

22. Kaneko, A.; Tamada, Y.; Hirai, S.; Kuzuya, T.; Hashimoto, T. Characterization of a silk-resinified compact fabricated using a pulse-energizing sintering device. *Macromol. Mater. Eng.* **2012**, *297*, 272–278, doi:10.1002/mame.201100112.
23. Bucciarelli, A.; Chiera, S.; Quaranta, A.; Yadavalli, V.K.; Motta, A.; Maniglio, D. A Thermal-Reflow-Based Low-Temperature, High-Pressure Sintering of Lyophilized Silk Fibroin for the Fast Fabrication of Biosubstrates. *Adv. Funct. Mater.* **2019**, *29*, 1901134, doi:10.1002/adfm.201901134.
24. Guo, C.; Li, C.; Vu, H. V.; Hanna, P.; Lechtig, A.; Qiu, Y.; Mu, X.; Ling, S.; Nazarian, A.; Lin, S.J.; et al. Thermoplastic moulding of regenerated silk. *Nat. Mater.* **2020**, *19*, 102–108, doi:10.1038/s41563-019-0560-8.
25. Marelli, B.; Patel, N.; Duggan, T.; Perotto, G.; Shirman, E.; Li, C.; Kaplan, D.L.; Omenetto, F.G. Programming function into mechanical forms by directed assembly of silk bulk materials. *Proc. Natl. Acad. Sci.* **2017**, *114*, 451–456, doi:10.1073/pnas.1612063114.
26. Guo, C.; Li, C.; Vu, H. V.; Hanna, P.; Lechtig, A.; Qiu, Y.; Mu, X.; Ling, S.; Nazarian, A.; Lin, S.; et al. Thermoplastic Molding of Regenerated Silk. *Nat. Mater.* **2020**, *19*, 102, doi:10.1038/S41563-019-0560-8.
27. Bucciarelli, A.; Janigro, V.; Yang, Y.; Fredi, G.; Pegoretti, A.; Motta, A.; Maniglio, D. A genipin crosslinked silk fibroin monolith by compression molding with recovering mechanical properties in physiological conditions. *Cell Reports Phys. Sci.* **2021**, *0*, doi:10.1016/J.XCRP.2021.100605.
28. Reddy, N.; Yang, Y. Citric acid cross-linking of starch films. *Food Chem.* **2010**, *118*, 702–711, doi:10.1016/j.foodchem.2009.05.050.
29. Raucci, M.G.; Alvarez-Perez, M.A.; Demitri, C.; Giugliano, D.; De Benedictis, V.; Sannino, A.; Ambrosio, L. Effect of citric acid crosslinking cellulose-based hydrogels on osteogenic differentiation. *J. Biomed. Mater. Res. Part A* **2015**, *103*, 2045–2056, doi:10.1002/jbm.a.35343.
30. Widsten, P.; Dooley, N.; Parr, R.; Capricho, J.; Suckling, I. Citric acid crosslinking of paper products for improved high-humidity performance. *Carbohydr. Polym.* **2014**, *101*, 998–1004, doi:10.1016/j.carbpol.2013.10.002.
31. Wu, H.; Lei, Y.; Lu, J.; Zhu, R.; Xiao, D.; Jiao, C.; Xia, R.; Zhang, Z.; Shen, G.; Liu, Y.; et al. Effect of citric acid induced crosslinking on the structure and properties of potato starch/chitosan composite films. *Food Hydrocoll.* **2019**, *97*, 105208, doi:10.1016/j.foodhyd.2019.105208.
32. Gawish, S.M.; Abo El-Ola, S.M.; Ramadan, A.M.; Abou El-Kheir, A.A. Citric acid used as a crosslinking agent for the grafting of chitosan onto woolen fabric. *J. Appl. Polym. Sci.* **2012**, *123*, 3345–3353, doi:10.1002/app.33873.
33. Stone, S.A.; Gosavi, P.; Athauda, T.J.; Ozer, R.R. In situ citric acid crosslinking of alginate/polyvinyl alcohol electrospun nanofibers. *Mater. Lett.* **2013**, *112*, 32–35, doi:10.1016/j.matlet.2013.08.100.
34. Awadhiya, A.; Kumar, D.; Verma, V. Crosslinking of agarose bioplastic using citric acid. *Carbohydr. Polym.* **2016**, *151*, 60–67, doi:10.1016/j.carbpol.2016.05.040.
35. Cumming, M.H.; Leonard, A.R.; LeCorre-Bordes, D.S.; Hofman, K. Intra-fibrillar citric acid crosslinking of marine collagen electrospun nanofibres. *Int. J. Biol. Macromol.* **2018**, *114*, 874–881, doi:10.1016/j.ijbiomac.2018.03.180.
36. Uranga, J.; Nguyen, B.T.; Si, T.T.; Guerrero, P.; de la Caba, K. The Effect of Cross-Linking with Citric Acid on the Properties of Agar/Fish Gelatin Films. *Polymers (Basel).* **2020**, *12*, 291, doi:10.3390/polym12020291.
37. Reddy, N.; Warner, K.; Yang, Y. Low-Temperature Wet-Cross-linking of Silk with Citric Acid. *Ind. Eng. Chem. Res.* **2011**, *50*, 4458–4463, doi:10.1021/ie102226f.
38. Khan, M.M.R.; Tsukada, M.; Gotoh, Y.; Morikawa, H.; Freddi, G.; Shiozaki, H. Physical properties and dyeability of silk fibers degummed with citric acid. *Bioresour. Technol.* **2010**, *101*, 8439–8445, doi:10.1016/j.biortech.2010.05.100.
39. Wang, W.; Pan, Y.; Gong, K.; Zhou, Q.; Zhang, T.; Li, Q. A comparative study of ultrasonic degumming of silk sericin using citric acid, sodium carbonate and papain. *Color. Technol.* **2019**, *135*, 195–201, doi:10.1111/cote.12392.
40. Xu, H.; Shen, L.; Xu, L.; Yang, Y. Low-temperature crosslinking of proteins using non-toxic citric acid in neutral aqueous medium: Mechanism and kinetic study. *Ind. Crops Prod.* **2015**, *74*, 234–240, doi:10.1016/j.indcrop.2015.05.010.
41. Bucciarelli, A.; Greco, G.; Corridori, I.; Pugno, N.M.; Motta, A. A Design of Experiment Rational Optimization of the Degumming Process and Its Impact on the Silk Fibroin Properties. *ACS Biomater. Sci. Eng.* **2021**, *7*, 1374–1393, doi:10.1021/acsbiomaterials.0c01657.

42. Bucciarelli, A.; Greco, G.; Corridori, I.; Motta, A.; Pugno, N.M. Tidy dataset of the experimental design of the optimization of the alkali degumming process of Bombyx mori silk. *Data Br.* **2021**, *38*, 107294, doi:10.1016/J.DIB.2021.107294.
43. Hu, X.; Kaplan, D.; Cebe, P. Determining Beta-Sheet Crystallinity in Fibrous Proteins by Thermal Analysis and Infrared Spectroscopy. *Macromolecules* **2006**, *39*, 6161–6170, doi:10.1021/ma0610109.
44. Um, I.C.; Kweon, H.Y.; Lee, K.G.; Park, Y.H. The role of formic acid in solution stability and crystallization of silk protein polymer. *Int. J. Biol. Macromol.* **2003**, *33*, 203–213, doi:10.1016/j.ijbiomac.2003.08.004.
45. Bucciarelli, A.; Pal, R.K.; Maniglio, D.; Quaranta, A.; Mulloni, V.; Motta, A.; Yadavalli, V.K. Fabrication of Nanoscale Patternable Films of Silk Fibroin Using Benign Solvents. **2017**, *201700110*, 1–9, doi:10.1002/mame.201700110.
46. Bucciarelli, A.; Mulloni, V.; Maniglio, D.; Pal, R.K.; Yadavalli, V.K.; Motta, A.; Quaranta, A. A comparative study of the refractive index of silk protein thin films towards biomaterial based optical devices. *Opt. Mater. (Amst).* **2018**, *78*, 407–414, doi:10.1016/j.optmat.2018.02.058.